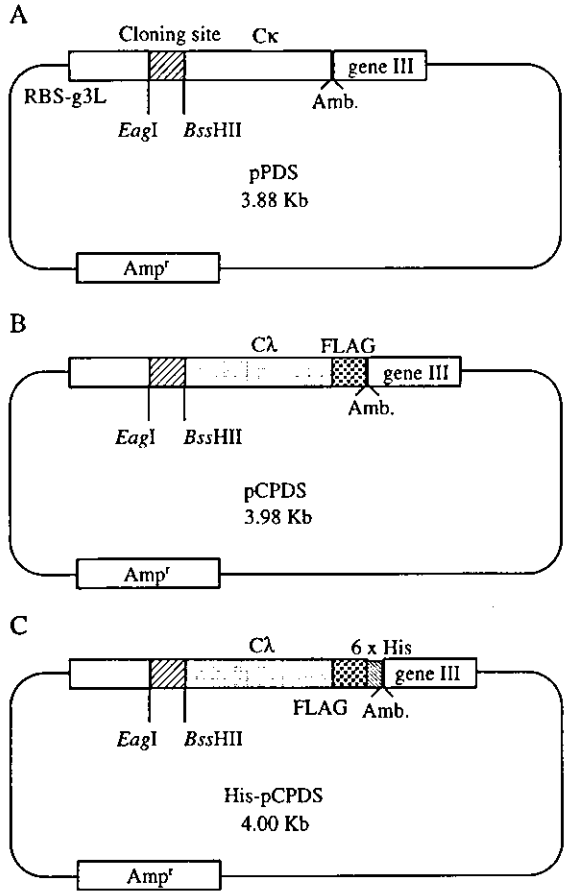

Fig. 1. Structure of the expression vectors ((A) pPDS, Yamanaka et al., 1995; (B) pCPDS; and (C) His-pCPDS). RBS-g3L: ribosomal binding site and leader sequence of cp3; Cκ: mouse Cκ sequence; Cλ: chicken Cλ sequence; FLAG: FLAG sequence; 6 × His: histidine repeat sequence; Amb: amber stop codon (TAG).

scFv gene only reacted with the anti-chicken λ chain antibody (data not shown).

Western blotting was performed to determine whether the scFv mAbs from the two vectors (HUC2s-1 and HUC2s-2) expressed the FLAG sequence. The HUC2s-1 and HUC2s-2 showed a single band of approximately 38–40 kDa, which is in agreement with the predicted size of the antibody-construct including the detection tag (Fig. 2A). HUC2s with the mouse Cκ was only detected by the anti-mouse κ antibody, as expected. These results showed that HUC2s-1 and HUC2s-2 expressed the FLAG tag, and that the incorporated stop codon was recognized correctly.

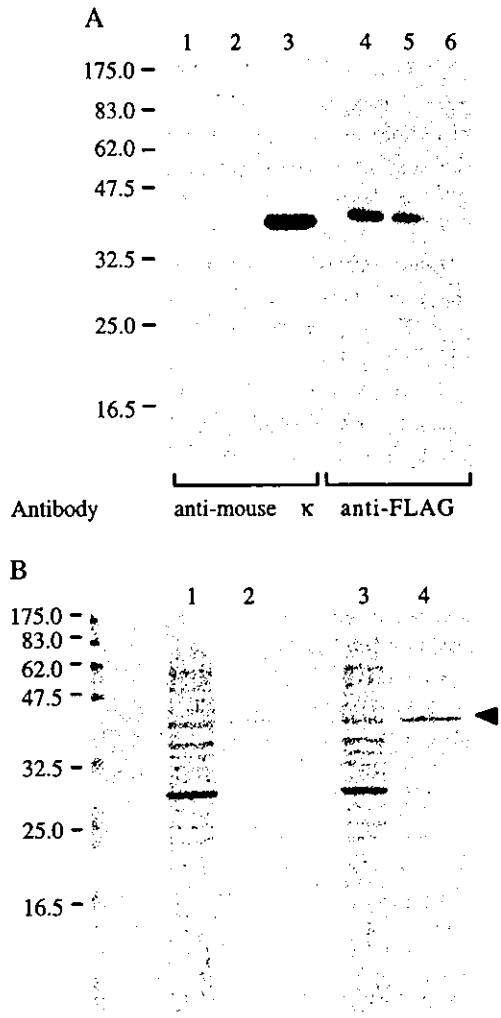

Fig. 2. Detection of recombinant chicken scFv mAbs. (A) Western blotting analysis of recombinant chicken mAbs, HUC2s-1 (lanes 1 and 4), HUC2s-2 (lanes 2 and 5) and HUC2s (lanes 3 and 6). The mAbs were separated in a 15% SDS-polyacrylamide gel and blotted onto PVDF membrane. The antibodies were detected with a peroxidase-labeled anti-mouse κ antibody (lanes 1–3) or a biotin-labeled anti-FLAG antibody and an ABC kit (Vector Laboratories, USA) (lanes 4–6). The numbers on the left represent the apparent molecular masses in kDa. (B) Purification of recombinant mAbs, HUC2s-1 (lanes 1 and 2) and HUC2s-2 (lanes 3 and 4). The arrow indicates the objective band. Lanes 1 and 3, unpurified bacterial supernatant; Lanes 2 and 4, HUC2s-1 and HUC2s-2, respectively, purified using the two-step method. The numbers on the left represent the apparent molecular masses in kDa.

3.3. Purification of recombinant scFv mAb

HUC2s-1 and HUC2s-2 were purified by anti-FLAG or nickel-chelating affinity chromatography, and ultimately purified using gel-chromatography. Yields were 1.743 mg/l culture supernatant after purification using the anti-FLAG column and gel-chromatography, and 1.197 mg/l culture supernatant after purification using the nickel-chelating affinity column and gel-chromatography. Purified mAbs were detected as a single band that corresponded to the molecular weights obtained in Western blotting (Fig. 2B). Although the purified mAbs showed dose-dependent reactivity with the H25 peptide antigen by ELISA, the concentration of the 1/2 maximal signal (optical density) of HUC2s-1 purified by anti-FLAG affinity chromatography was about 10-fold lower that that of HUC2s-2 purified by nickel-chelating affinity chromatography (Fig. 3). The optical density of the original HUC2-13 treated with 0.1 M glycine–HCl (pH 2.2) at 30 min was also lower than that of the non-treated HUC2-13 (unpublished data). These results show that the HUC2-13 scFv form was more sensitive to acid conditions than the intact form of HUC2-13 and that it is necessary to maintain neutral pH conditions during scFv mAb purification.

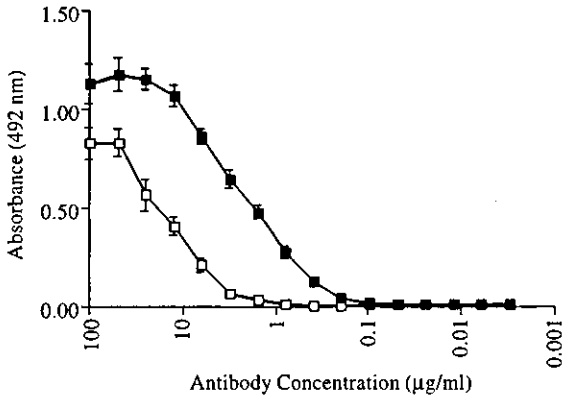

Fig. 3. ELISA analysis of the purified scFv antibodies. Two-fold serially diluted scFv mAbs were reacted with the H25 peptide. Absorbance of the mAb from pCPDS (HUC2s-1) is represented by open squares and that of the mAb from His-pCPDS (HUC2s-2) is represented by closed squares. Data represent the mean ± S.D., $n=3$ wells/experiment.

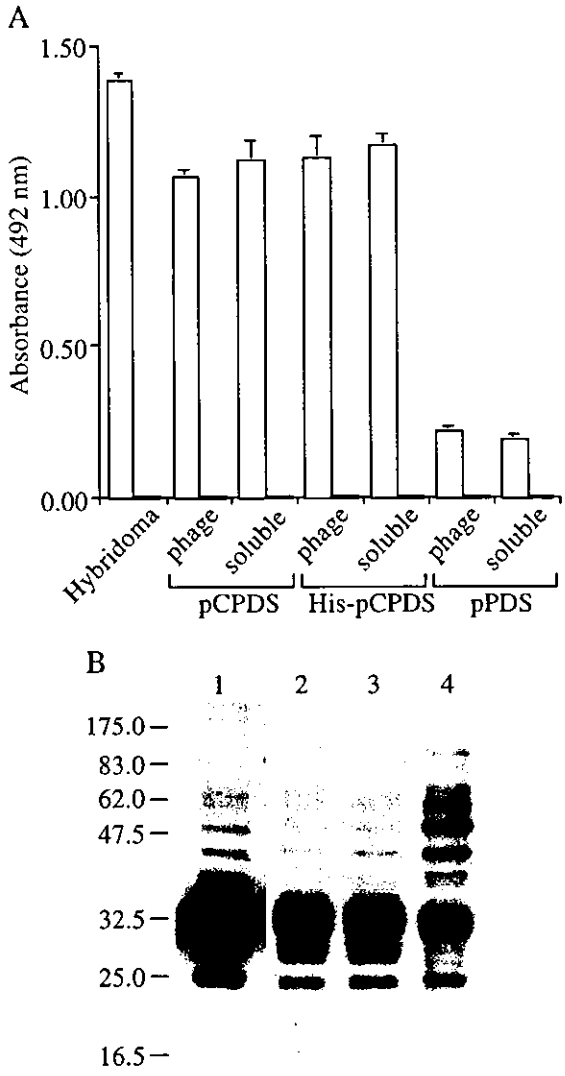

Fig. 4. Functional analysis of recombinant mAbs. (A) Binding specificity of recombinant HUC2-13 scFv. Open bars represent the H25 peptide. Solid bars represent the BSA antigen. Data represent mean ± S.D., $n=3$ wells/experiment. (B) Western blotting analysis of mouse brain PrP^{c} using recombinant mAbs. Lane 1 was stained with the supernatant from a HUC2-13 hybridoma culture. Lanes 2, 3 and 4 were stained with the soluble mAbs HUC2s-1, HUC2s-2 and HUC2s, respectively. The numbers on the left represent the apparent molecular masses in kDa.

3.4. Functional analysis of recombinant scFv mAb

The specificity of the mAbs, the phage-displayed mAbs and soluble mAbs from the bacterial culture supernatant were determined by ELISA using synthetic human PrP peptide (H25) or BSA (control antigen) and Western blotting using mouse brain homogenates. The phage-displayed mAbs (HUC2p-1 and HUC2p-2) and the soluble mAbs (HUC2s-1 and HUC2s-2), as well as the culture supernatant of the HUC2-13 hybridoma, were shown to bind specifically to H25 (Fig. 4A). The low reactivity of scFv from pPDS was because the anti-chicken λ secondary antibody could only recognize Vλ of the HUC2-13 scFv. In Western blotting, HUC2s-1, HUC2s-2, HUC2s and intact HUC2-13 showed three bands of PrP due to differences in the glycosylation (Prusiner et al., 1998) (Fig. 4B). The signal intensities of HUC2s-1 and HUC2s-2 were greater than that of HUC2s. Background staining was minimal with HUC2s-1 or HUC2s-2 when compared with HUC2s.

The scFv has the chicken Cλ chain, and thus it is not necessary to use an antibody against the specific tag for detection; it can be detected as a chicken antibody. This scFv can also be applied to two-antibody assay systems together with other chicken antibodies, if an antibody against FLAG or the 6 ×His tag is used for detection. In conclusion, we have established two new vectors (pCPDS and His-pCPDS) for the production of recombinant chicken scFv antibodies having the same binding specificity as the original antibody. The present results may provide an alternative to chicken mAb production from hybridomas and immunized-chicken splenocytes as well as contribute to the more widespread use of chicken mAb reagents in numerous fields.

Acknowledgements

The authors wish to thank Dr. Yamanaka, I.H. (Rohto Pharmaceutical, Japan) for kindly providing the pPDS vector and generously dispensing technical advice. This work was partly supported by a Grant-in-Aid for Exploratory Research from the Ministry of Education, Science and Culture, a Grant-in-Aid (Research Project for Studies on the Pathogenesis of Prion Disease) from the Ministry of Agriculture, Forestry and Fisheries, a Grant-in-Aid from the Bio-oriented Technology Research Advancement Institution (BRAIN), and the Japan Society for the Promotion of Science (JSPS).

References

Asaoka, H., Nishinaka, S., Wakamiya, N., Matsuda, H., Murata, M., 1992. Two chicken monoclonal antibodies specific for heterophil Hanganutziu-Deicher antigen. Immunol. Lett. 32, 91.

Bernard, O., Hozumi, N., Tonegawa, S., 1978. Sequences of murine immunoglobulin light chain genes before and after somatic changes. Cell 15, 1133.

Brizzard, B.L., Chubet, R.G., Vizard, D.L., 1994. Immunoaffinity purification of FLAG epitope-tagged bacterial alkaline phosphatase using a novel monoclonal antibody and peptide elution. Biotechniques 16, 730.

Burton, D.R., Barbas III, C.F., Persson, M.A.A., Koenig, S., Chanock, R.M., Lerner, R.A., 1991. A large array of human monoclonal antibodies to type 1 human immunodeficiency virus from combinatorial libraries of asymptomatic seropositive individuals. Proc. Natl. Acad. Sci. U. S. A. 88, 10134.

Davies, E.L., Smith, J.S., Birkett, C.R., Manser, J.M., Anderson-Dear, D.V., Young, J.R., 1995. Selection of specific phage-display antibodies using libraries derived from chicken immunoglobulin genes. J. Immunol. Methods 186, 125.

Groschup, M.H., Harmeyer, S., Pfaff, E., 1997. Antigenic features of prion proteins of sheep and of other mammalian species. J. Immunol. Methods 207, 89.

Hadge, D., Ambrosius, H., 1984. Evolution of low molecular weight immunoglobulins: IV. IgY-like immunoglobulins of birds, reptiles and amphibians, precursors of mammalian IgA. Mol. Immunol. 21, 699.

Hoogenboom, H.R., Griffiths, A.D., Johnson, K.S., Chiswell, D.J., Hudson, P., Winter, G., 1991. Multi-subunit proteins on the surface of filamentous phage: methodologies for displaying antibody (Fab) heavy and light chains. Nucl. Acids Res. 19, 4133.

Jennifer, A.W., Rader, C., Steinberger, P., Fuller, R., Barbas III, C.F., 2000. Methods for the generation of chicken monoclonal antibody fragments by phage display. J. Immunol. Methods 242, 159.

Marks, J.D., Hoogenboom, H.R., Bonnert, T.P., McCafferty, J., Griffiths, A.D., Winter, G., 1991. By-passing immunization. Human antibodies from V-gene libraries displayed on phage. J. Mol. Biol. 222, 581.

Matsuda, H., Mitsuda, H., Nakamura, N., Furusawa, S., Mohri, S., Kitamoto, T., 1999. A chicken monoclonal antibody with specificity for the N-terminal of human prion protein. FEMS Immunol. Med. Microbiol. 23, 189.

Matsushita, K., Horiuchi, H., Furusawa, S., Horiuchi, M., Shinagawa, M., Matsuda, H., 1998. Chicken monoclonal antibodies against synthetic bovine prion protein peptide. J. Vet. Med. Sci. 60, 777.

McCormack, W.T., Thompson, C.B., 1990. Chicken IgL variable region gene conversions display pseudogene donor preference and 5′ to 3′ polarity. Gene Dev. 4, 548.

Nakamura, N., Aoki, Y., Horiuchi, H., Furusawa, S., Yamanaka, I.H., Kitamoto, T., Matsuda, H., 2000. Construction of recombinant monoclonal antibodies from a chicken hybridoma line secreting specific antibody. Cytotechnology 32, 191.

Nishida, N., Harris, D.A., Vilette, D., Laude, H., Frobert, Y., Grassi, J., Casanova, D., Milhavet, O., Lehmann, S., 2000. Successful transmission of three mouse-adapted scrapie strains to murine neuroblastoma cell lines overexpressing wild-type mouse prion protein. J. Virol. 74, 320.

Nishinaka, S., Akiba, H., Nakamura, M., Suzuki, K., Suzuki, T., Tsubokura, K., Horiuchi, H., Furusawa, S., Matsuda, H., 1996. Two chicken B cell lines resistant to ouabain for the production of chicken monoclonal antibodies. J. Vet. Med. Sci. 58, 1053.

Prusiner, S.B., Scott, M.R., DeArmond, S.J., Cohen, F.E., 1998. Prion protein biology. Cell 93, 337.

Reynaud, C.A., Anquez, V., Dahan, A., Weill, J.C., 1985. A single rearrangement event generates most of the chicken immunoglobulin light chains diversity. Cell 40, 283.

Reynaud, C.A., Anquez, V., Grimal, H., Weill, J.C., 1987. A hyperconversion mechanism generates the chicken light chain preimmune repertoire. Cell 48, 379.

Reynaud, C.A., Dahan, A., Anquez, V., Weill, J.C., 1989. Somatic hyperconversion diversifies the single VH gene of the chicken with a high incidence in the D region. Cell 59, 171.

Sakano, H., Maki, R., Kurosawa, Y., Roeder, W., Tonegawa, S., 1980. Two types of somatic recombination are necessary for the generation of complete immunoglobulin heavy-chain genes. Nature (Lond.) 286, 676.

Shimizu, M., Nagashima, H., Sano, K., Hashimoto, K., Ozeki, M., Tsuda, K., Hatta, H., 1992. Molecular stability of chicken and rabbit immunoglobulin G. Biosci. Biotechnol. Biochem. 56, 270.

Song, C.S., Yu, J.H., Bai, D.H., Hester, P.Y., Kim, K.H., 1985. Antibodies to the alpha-subunit of insulin receptor from the eggs of immunized hens. J. Immunol. 135, 3354.

Thompson, C.B., Neiman, P.E., 1987. Somatic diversification of the chicken immunoglobulin light chain gene is limited to the rearranged variable gene segment. Cell 48, 369.

Yamanaka, I.H., Kirii, Y., Ohmoto, H., 1995. An improved phage display antibody cloning system using newly designed PCR primers optimized for *pfu* DNA polymerase. J. Biochem. 117, 1218.

Yamanaka, I.H., Inoue, T., Ikeda-Tanaka, O., 1996. Chicken monoclonal antibody isolated by a phage display. J. Immunol. 157, 1156.

HYBRIDOMA AND HYBRIDOMICS
Volume 22, Number 4, 2003

Short Communication

Generation of Antibodies Against Prion Protein by Scrapie-Infected Cell Immunization of $PrP^{0/0}$ Mice

NAOTO NAKAMURA,[1] KAZUYOSHI MIYAMOTO,[1] MARIKO SHIMOKAWA,[1] NORIUKI NISHIDA,[2] SHIROU MOHRI,[3] TETSUYUKI KITAMOTO,[4] HIROYUKI HORIUCHI,[1] SHUICHI FURUSAWA,[1] and HARUO MATSUDA[1]

ABSTRACT

Four monoclonal antibodies (MAbs) specific for prion protein (PrP) were generated by using PrP-knockout mice immunized with a scrapie-infected mouse neuroblastoma cell line (N2a/22L). The MAbs reacted with both the cellular form (PrP^C) and the protease K-treated form (PrP^{Sc}) on Western blotting. Of the four MAbs, three recognized mouse and hamster PrP, while the remaining MAb recognized mouse, sheep, and bovine PrPs. In addition, these MAbs were shown to react only with the unglycosylated and monoglycosylated forms of PrP^{Sc} in N2a/22L, but reacted with all glycosylated forms of PrP^C and PrP^{Sc} from mouse brain. This study was the first to report the development of anti-PrP MAbs using scrapie-infected cells as an immunogen and provides one approach for the generation of PrP-specific MAbs.

THE TRANSMISSIBLE SPONGIFORM ENCEPHALOPATHIES (TSEs) are a group of fatal neurodegenerative disorders that include Creutzfeldt-Jacob disease (CJD) in humans, scrapie in sheep and goats, and bovine spongiform encephalopathies (BSEs).[1] These disorders are believed to occur through the accumulation of an abnormal pathogenic prion protein isoform (PrP^{Sc}) that is converted from cellular PrP (PrP^C). The PrP^{sc} possesses some protease K (PK) resistance, whereas PrP^C is completely digested by PK.[2–4]

Final confirmatory diagnoses of TSEs as well as the study of basic prion biology and their pathogenesis require the use of PrP-specific antibodies.[5,6] Although numerous groups attempted to generate PrP-specific monoclonal antibodies (MAbs), the high homology (>84%) among mammalian PrP amino acid sequences limited development of such MAbs.[4] As a result, a limited number of the MAbs are available for detecting PrPs of different origins.[7,8] To circumvent this immunotolerance in laboratory animals immunized with PrP, $PrP^{0/0}$ mice, which lack PrP tolerance characteristics, are used for the production of PrP-specific MAbs. Numerous PrP-specific MAbs have been raised using $PrP^{0/0}$ mice immunized with recombinant PrPs,[6,9] synthetic PrP peptides,[10] DNA encoded PrP,[11] or purified scrapie-associated fibril (SAF).[12] However, it is difficult to prepare these immunogens in sufficient volume. On the other hand, scrapie-infected cell lines, such as ScN2a[13] or N2a/22L,[14] may have the same immunogenic effects against $PrP^{0/0}$ mice as immunization with intact forms of PrP^{Sc} and PrP^C, because these cell lines are of mouse origin and the $PrP^{0/0}$ mice will show the immunotolerance against cellular components other than PrP.

In this study, four MAbs specific for PrP were generated by using $PrP^{0/0}$ mice immunized with N2a/22L cells. The MAbs reacted with both PrP^C and PrP^{Sc} on Western blotting. Of the four MAbs, three recognized mouse and hamster PrP, while the remaining MAb recognized mouse, sheep and bovine PrPs. In addition, these MAbs were shown to react only with the un-

[1]Laboratory of Immunobiology, Department of Molecular and Applied Bioscience, Graduate School of Biosphere Science, Hiroshima University, Higashi-Hiroshima, Japan.
[2]Department of Molecular Microbiology and Immunology, Graduate School of Medical Sciences, Nagasaki University, Nagasaki, Japan.
[3]Laboratory of Biomedicine, Center of Biomedical Research, Graduate School of Medical Sciences, Kyushu University, Higashi-ku, Fukuoka, Japan.
[4]Department of Neurological Science, Graduate School of Medicine, Tohoku University, Aoba-ku, Sendai, Japan.

glycosylated and monoglycosylated forms of PrP^{Sc} in N2a/22L, but reacted with all glycosylated forms of PrP^{C} and PrP^{Sc} from mouse brain. This study is the first report on the development of anti-PrP MAbs using scrapie-infected cells as an immunogen and will provide one approach for the generation of PrP-specific MAbs. We herein report the first successful immunization of $PrP^{0/0}$ mice with the N2a/22L cell line, which expresses more PrP^{Sc} and is more stable than ScN2a, and the establishment of MAbs against PrP.

Monoclonal antibodies were generated by conventional cell fusion technology. Briefly, 6-week-old $PrP^{0/0}$ mice[15] were immunized intraperitonealy (i.p.) with N2a/22L (2.0×10^6 cells per body). The mice received five additional i.p. injections of the corresponding antigen at 3-week intervals. Three days after the final boost, the splenocytes from the immunized-mice were fused with the SP2/0-Ag14 cells (SP2).[16] Cell fusion was carried out at SP2/splenocytes ratio of 1:5 in 50% (w/v) polyethylene glycol 1500 (Roche Diagnostics, Mannheim, Germany) and selected in HAT medium. The supernatants were screened by ELISA using recombinant PrPs. In the determination of specificity of the mAbs, various recombinant PrP peptides were used. The ELISA plates (Maxisorp, Nunc, New York) were coated with 50 μL/well (2.5 μg/well) of various recombinant PrP peptides and washed and blocked with 350 μL/well of PBS containing 25% BlockAce (Yukijirushi, Japan) at 37°C for 2 h. The hybridoma culture supernatants were then added to each well (50 μL/well) and were incubated at 37°C for 1 h. The specific MAbs were detected using a peroxidase-labeled anti-mouse Ig antibody (Kirkegaard and Perry Laboratories, Gaithersburg, MD). After washing the plates, *o*-phenylene diamine sulfate (Sigma, St. Louis, MO) was added and the optical density was measured at 492 nm. Recombinant PrP fragments, M23-231, M23-87, M23-167, M23-214, M89-231, M155-231 (mouse PrP: codon 23-231, 23-87, 23-167, 23-214, 89-231 and 155-231) and Ha23-231 (hamster PrP: codon 23–231) were kindly supplied by Dr. Horiuchi (Obihiro Univ. Agric. Vet. Med. Japan). Recombinant PrP fragment, H122-230 (human PrP: codon 122-230), M121-231 (mouse PrP: codon 121-231), S125-234 (sheep PrP: codon 125-234) and B133-241 (bovine PrP: codon 133-241) were generated with pET22b (Novagen, Darmstadt, Germany), and purified with nickel ion-charged Chelating Sepharose Fast Flow (Amersham Biosciences, Sweden) and HiPrep Sephacryl S-100 HR (Amersham Biosciences, Uppsala, Sweden) according to manufacturers' instructions. Synthetic mouse PrP peptides (M53-68, M69-84, M85-100, M94-109, M109-127, M124-144, M141-159, M156-175, M172-181, M182-190, M187-204, M205-224 and M220-242) were synthesized by a solid-phase peptide synthesizer system Model PSSM-8 (Shimazu, Kyoto, Japan).

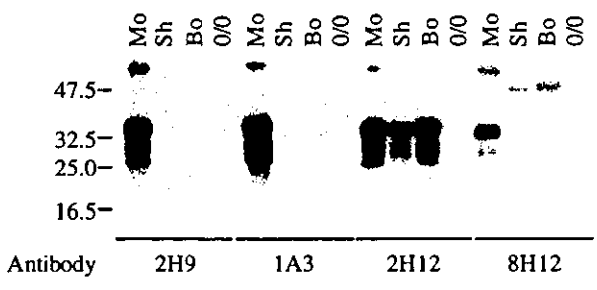

FIG. 1. Western blot profiles of mouse, sheep, and bovine PrP^{C} using PrP-specific mouse monoclonal antibodies. Color development was performed using a peroxidase/ECL system. Mo, Sh, Bo, and 0/0: wild mouse, sheep, bovine, and $PrP^{0/0}$ mouse brain homogenate, respectively. The numbers at the left represent the apparent molecular masses in kDa.

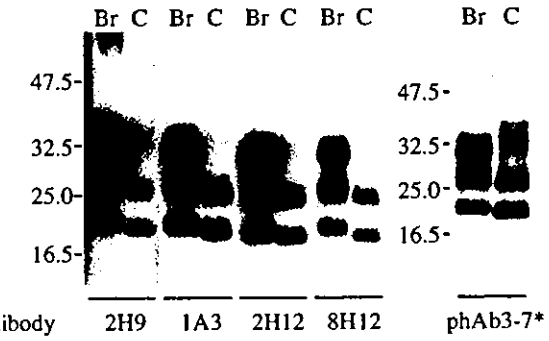

FIG. 2. Western blot profiles of PK-treated mouse PrP^{Sc} using PrP-specific mouse monoclonal antibodies. Color development was performed using a peroxidase/ECL system. Br, scrapie infected-mouse brain; C, N2a/22L. The numbers at the left represent the apparent molecular masses in kDa. *The phAb3-7 recognizing mouse PrP 90-110 amino acid residues was used as a positive control.

Positive hybridoma cells were cloned by limiting dilution. Subclassification of the antibodies was carried out using a mouse MAb isotyping kit (Amersham Biosciences, Sweden). Some hybridoma cells exhibited diminution of PrP-specific Ab secretion and cell-death, as reported previously.[17] Four hybridoma clones producing specific antibody were subsequently identified. Thee MAbs, named 22L/2H9 (2H9), 22L/1A3 (1A3), 22L/2H12 (2H12) and 22L/8H12 (8H12), were classified as IgG_1/κ, except for 8H12, which was IgM/κ (data not shown).

The epitopes of these MAbs were determined by ELISA using recombinant mouse PrPs of various regions. The MAbs 2H9 and 1A3 reacted with M23-231, M89-231, and M121-231, and the mAbs 2H12 and 8H12 reacted with M23-231, M89-231, M121-231 and M155-231. None of the MAbs showed reactivity against the three C-terminus truncated-mouse PrPs (M23-87, M23-167 and M23-214) or the 13 overlapping peptides derived from the mouse PrP sequence. These results indicated that the four MAbs bind to discontinuous epitopes, and that the C-terminus of the PK-resistant core region (codon 121–231) is an important site for MAb recognition. Moreover, it showed that antigen presentation was dependent on maintaining an intact PrP conformation. In the present study, none of the MAbs recognized the PK-sensitive regions of PrPs developed by cell fusion.

The cross-reactivity of the four MAbs with mammalian PrPs was assessed by ELISA using recombinant mouse, hamster, human, sheep and bovine PrPs. The MAbs 2H9, 1A3 and 8H12 reacted with mouse and hamster PrPs, while the mAb 2H12 reacted with mouse, sheep and bovine PrPs. None of the MAbs reacted with human PrP.

In Western blotting analysis, normal brain tissues from Balb/c mouse, sheep, and bovine, as well as brain tissue from $PrP^{0/0}$ mouse were homogenized in 9 vol of lysis buffer (10

mM Tris [pH 7.5], 100 mM NaCl, 1 mM EDTA, 0.5% Triton-X100, 0.5% sodium deoxycholate) containing a protease inhibitor cocktail (Roche Diagnostics). Homogenates were centrifuged at 800 × *g* for 5 min. Protein concentration in the supernatant was measured with the *DC* protein assay kit (Bio-Rad, Hercules, CA). The equivalent of 50 μg total protein under non-reducing conditions was separated on a 13.5% polyacrylamide gel and then transferred to an Immun-Blot™ PVDF membrane (Bio-Rad) at 200 mA for 2 h. The membranes were then incubated for 1 h at room temperature with the different MAbs, developed by peroxidase-conjugated anti-mouse Ig antibodies and the ECL (Amersham Biosciences, Sweden), and then exposed on x-ray film RX-U (FujiFilm, Tokyo, Japan) for 3 min.

Mouse PrP^{Sc} was prepared from scrapie-infected mouse brain (kindly supplied by Dr. Yokoyama of the NIAH, Japan) and N2a/22L. Preparation of PK-treated PrP^{Sc} from brain and N2a/22L was conducted as described previously.[14,15] These samples were separated on a 13.5% polyacrylamide gel and blotted as described above.

Western blot analysis was used to confirm the reactivity of these four MAbs with PrP^{C} and PrP^{Sc}. Figure 1 shows the detection of PrP^{C} in mouse, sheep and bovine brain tissues by MAbs 2H9, 1A3, 2H12 and 8H12. The mAbs 2H9, 1A3 and 8H12 recognized mouse PrP, but failed to react with sheep and bovine PrPs. The MAb 2H12 recognized mouse, sheep and bovine PrPs. None of the MAbs reacted with the brain homogenate from $PrP^{0/0}$ mouse, confirming the specificity of all the MAbs for PrP. Moreover, the reactivity of 2H9 and 1A3 against PrP decreased under reducing conditions (data not shown). This result indicated that the epitopes for 2H9 and 1A3 formed an intramolecular disulfide bond with PrP.

Figure 2 shows the detection of PrP^{Sc} in scrapie-infected mouse brain and N2a/22L cell line. All of the MAbs reacted equally with all three glycoforms of PrP^{Sc} in infected mouse brain; however, these MAbs failed to recognize the diglycosylated form of PrP^{Sc} in N2a/22L. This may be due to differences in the PrP^{Sc} between infected mice and N2a/22L cells. In Western blot analysis of PrP^{Sc} from mouse brain and N2a/22L using chicken anti-PrP recombinant MAb phAb3-7 (epitope; mouse PrP codon 97-100, Nakamura et al., in preparation), the PrP^{Sc} profiles of N2a/22L could be distinguished from those of infected-mouse brain by differences in the size of the unglycosylated fragment and the mobility of the diglycosylated fragment, as reported previously.[14] This result supports the theory that the glycosylation of the PrP^{Sc} depends not only upon the strain but also on the host cell type.[18]

The scrapie-infected N2a/22L cell line for immunization against $PrP^{0/0}$ mice was effective for the production of PrP-specific MAbs. This is because the cells are of mouse origin and $PrP^{0/0}$ mice will only respond to intact forms of expressed PrP.

In conclusion, we attempted to produce PrP-specific MAbs using a scrapie-infected cell line as an immunogen against $PrP^{0/0}$ mice, and established four MAbs able to detect PrP in Western blotting. In this study, although these antibodies could not distinguish between PrP^{C} and PrP^{Sc} (data not shown), it was suggested that this immunization strategy might be useful for producing antibodies that can recognize the various PrP isoforms. Furthermore, if scrapie strain-specific MAbs can be developed by immunization with infected cell line that maintain the properties of the scrapie strains, the progression of research into the molecular mechanisms behind strain variation would be greatly facilitated.

ACKNOWLEDGMENTS

We are grateful to Dr. M. Horiuchi (Obihiro Univ., Agric. Vet. Med., Japan) for providing recombinant mouse and hamster PrPs, and to Dr. T. Yokoyama (NIAH, Japan) for infected brain homogenate. This work was partly supported by a Grant-in-Aid from the Ministry of Health, Labour and Welfare, a Grant-in-Aid from the Ministry of Agriculture, Forestry and Fisheries, a Grant-in-Aid from the Bio-oriented Technology Research Advancement Institution (BRAIN), and the Japan Society for the Promotion of Science (JSPS).

REFERENCES

1. Prusiner SB, Scott MR, DeArmond SJ, and Cohen FE. Prion protein biology. Cell 1998;93:337–348.
2. Prusiner SB, McKinley MP, Bowman KA, Bolton DC, Bendheim PE, Groth DF, and Glenner GG: Scrapie prions aggregate to form amyloid-like birefringent rods. Cell 1983;35:349–358.
3. Meyer RK, McKinley MP, Bowman KA, Braunfeld MB, Barry RA, and Prusiner SB: Separation and properties of cellular and scrapie prior proteins. Proc Natl Acad Sci USA 1986;83: 2310–2314.
4. Oesch B, Westaway D, Walchli M, McKinley MP, Kent SBH, Aebersold R, Barry RA, Tempst P, Teplow DB, and Hood LE: A cellular gene encodes scrapie PrP 27-30 protein. Cell 1985;40: 735–746.
5. Singh N, Zanusso G, Chen SG, Fujita H, Richardson S, Gambetti P, Petersen RB: Prion protein aggregation reverted by low temperature in transfected cells carrying a prion protein gene mutation. J Biol Chem 1997;272:28461–28470.
6. Zanusso G, Liu D, Ferrari S, et al: Prion protein expression in different species: analysis with a panel of new mAbs. Proc Natl Acad Sci USA 1998;95:8812–8816.
7. Barry RA, and Prusiner SB: Monoclonal antibodies to the cellular and scrapie prion proteins. J Infect Dis 1986;154:518–521.
8. Kascsak RJ, Rubenstein R, Merz PA, Tonna DeMasi M, Fersko R, Carp RI, Wisniewski HM, and Diringer H: Mouse polyclonal and monoclonal antibody to scrapie-associated fibril proteins. J Virol 1987;61:3688–3693.
9. Korth C, Stierli B, Streit P, Moser M, Schaller O, Fischer R, Schulz-Schaeffer W, Kretzschmar H, Raeber A, Braun U, Ehrensperger F, Hornemann S, Glockshuber R, Riek R, Billeter M, Wuthrich K, and Oesch B: Prion (PrP^{sc})-specific epitope defined by a monoclonal antibody. Nature 1997;398:74–77.
10. Harmeyer S, Pfaff E, and Groschup MH: Synthetic peptide vaccines yield monoclonal antibodies to cellular and pathological prion proteins of ruminants. J Gen Virol 1998;79:937–945.
11. Krasemann S, Groschup M, Hunsmann G, and Bodemer W: Induction of antibodies against human prion proteins (PrP) by DNA-mediated immunization of $PrP^{0/0}$ mice. J Immunol Methods 1996;199:109–118.
12. Demart S, Fournier JG, Creminon C, Frobert Y, Lamoury F, Marce D, Lasmezas C, Dormont D, Grassi J, and Deslys JP: New insight into abnormal prion protein using monoclonal antibodies. Biochem Biophys Res Commun 1999;265:652–657.
13. Caughey B, Race RE, Ernst D, Buchmeier MJ, and Chesebro B:

Prion protein biosynthesis in scrapie-infected and uninfected neuroblastoma cells. J Virol 1989;63:175–181.
14. Nishida N, Harris DA, Vilette D, Laude H, Frobert Y, Grassi J, Casanova D, Milhavet O, and Lehmann S: Successful transmission of three mouse-adapted scrapie strains to murine neuroblastoma cell lines overexpressing wild-type mouse prion protein. J Virol 2000;74:320–325.
15. Yokoyama T, Kimura MK, Ushiki Y, Yamada S, Morooka A, Nakashiba T, Sassa T, and Itohara S: In Vivo conversion of cellular prion protein pathogenic isoforms, as monitored by conformation-specific antibodies. J Biol Chem 2001;276:11265–11271.
16. Shulman M, Whide CD, and Kohler G: A better cell line for making hybridomas screting specific antibodies. Nature 1978;276: 269–270.
17. Williamson RA, Peretz D, Smorodinsky N, Bastidas R, Serban H, Mehlhorn I, DeArmond SJ, Prusiner SB, and Burton DR: Circumventing tolerance to generate autologous monoclonal antibodies to the prior protein. Proc Natl Acad Sci USA 1996;93:7279–7282.
18. Somerville RA, Chong A, Mulqueen OU, Birkett CR, Wood SC, and Hope J: Biochemical typing of scrapie strains. Nature 1997;997:564.

Address reprint requests to:
H. Matsuda, D.V.M., Ph.D.
Laboratory of Immunobiology
Department of Molecular and Applied Bioscience
Graduate School of Biosphere Science
Hiroshima University
1-4-4 Kagamiyama
Higashi-Hiroshima 739-8528, Japan

E-mail: hmatsu@hiroshima-u.ac.jp

Received for publication April 29, 2003. Accepted for publication June 10, 2003.

Acta Neuropathol (2003) 105 : 462–468
DOI 10.1007/s00401-002-0667-9

REGULAR PAPER

Hitoshi Kikuchi · Takeshi Yamada · Hirokazu Furuya
Katsumi Doh-ura · Yasumasa Ohyagi · Toru Iwaki
Jun-ichi Kira

Involvement of cathepsin B in the motor neuron degeneration of amyotrophic lateral sclerosis

Received: 12 July 2002 / Revised: 9 December 2002 / Accepted: 11 December 2002 / Published online: 29 January 2003

Abstract Abnormal proteolysis may be involved in the motor neuron degeneration of amyotrophic lateral sclerosis (ALS). Although several studies of the ubiquitin-proteasome system in ALS have been reported, the endosome-lysosome system has not been investigated in detail. To clarify the association of neurodegeneration with the endosome-lysosome system in ALS, we examined the pathological expression of cysteine proteases such as cathepsins B, H and L and an aspartate protease, cathepsin D, in the anterior horns of 15 ALS cases and 5 controls. In the ALS cases, cathepsin B immunoreactivity was preferentially decreased in the lateral parts of the anterior gray horns compared with the controls. Its immunoreactivity was increased in the cytoplasm of both shrunken and pigmented neurons but was weak in the neurons containing Bunina bodies. In addition, reactive astrocytes were also immunolabeled with cathepsin B. Cathepsin H and cathepsin L were detected in the cytoplasm of a small number of shrunken and pigmented neurons. Cathepsin D immunoreactivity was strong in the cytoplasm of all motor neurons. The immunoreactivity of cathepsins H, L and D was not significantly different between control and ALS cases. Western blot analysis showed that the 25-kDa activated form of cathepsin B was down-regulated in ALS. Our results suggest that cathepsin B is involved in the motor neuron degeneration in ALS.

Keywords Amyotrophic lateral sclerosis · Cathepsin B · Bunina body · Spinal cord · Proteolysis

H. Kikuchi (✉) · T. Yamada · H. Furuya · Y. Ohyagi · J.-i. Kira
Department of Neurology, Neurological Institute,
Graduate School of Medical Sciences, Kyushu University,
812-8582 Fukuoka, Japan
e-mail: hk2068@columbia.edu

K. Doh-ura · T. Iwaki
Department of Neuropathology, Neurological Institute,
Graduate School of Medical Sciences, Kyushu University,
812-8582 Fukuoka, Japan

Introduction

Amyotrophic lateral sclerosis (ALS) is a human motor neuron disease characterized by the degeneration of both upper and lower motor neurons [32]. Various types of degenerative motor neurons, including shrunken, pigmented and chromatolytic neurons, as well as normal-appearing neurons, are seen in ALS [16]. Although several pathophysiological hypotheses such as oxidative stress, excitotoxins and cytoskeletal abnormalities [10, 14, 16, 18, 20, 22], have been proposed, the etiology of motor neuron degeneration in ALS is still unknown.

Recently, abnormal proteolysis associated with neuronal cell death has been reported in various neurodegenerative diseases such as Alzheimer's disease (AD) [2, 31]. ALS is also associated with the abnormal proteolysis of motor neurons [25, 30]. Various types of ubiquitinated inclusions, such as skein-like or spherical ones, are found in ALS motor neurons, which suggests that the ubiquitin-proteasome system is not well organized [25]. Among other proteolytic pathways, the endosome-lysosome system is noted as well because the cystatin C immunoreactivity increases in Bunina bodies, which are specific to ALS [30].

Bunina bodies are small eosinophilic intracytoplasmic inclusions that are observed exclusively in ALS motor neurons and are pathognomonic of ALS, but their origin is unknown [8]. Bunina bodies are immunolabeled with antibody against a cysteine protease inhibitor, cystatin C [30]. However, cysteine proteases such as cathepsins B, H and L, or the aspartate protease cathepsin D, which activates cathepsins B, H and L, have not been investigated in detail [4, 7, 30]. To clarify the association of neurodegeneration with the endosome-lysosome protease systems in ALS, we examined the expression of cathepsins B, H, L and D in the anterior horn cells in ALS.

Table 1 Summary of immunohistochemical results. Cathepsin B positivity of each neurons is given as: –, no cell; 0, none; +1, 0–25%; +2, 26–50%; +3, 51–75%; +4, above 75%. Neuronal loss: 0, no; +1, slight to mild; +2, moderate to severe. <separator/> Astrocytosis: 0, no; +1, slight to mild; +2, moderate to severe. Bunina body: 0, none; +, a few (1 per one section); +3, many (>4 per one section); +2, between +1 and +3 (*CC* cervical spinal cord, *LC* lumbar spinal cord, *LAG* lateral part of the anterior gray horn, *MAG* medial part of the anterior gray horn, *N* normal-appearing neuron, *S* shrunken neuron, *P* pigmented neuron, *C* chromatolytic neuron, *HCC* hepatocellular carcinoma, *CRF* chronic renal failure)

Case	Age/ sex	Duration (month)	Bunina body		Cathepsin B																Neuronal loss		Astrocytosis	
			CC	LC	CC								LC								CC	LC	CC	LC
					LAG				MAG				LAG				MAG							
					N	S	P	C	N	S	P	C	N	S	P	C	N	S	P	C				
Amyotrophic lateral sclerosis																								
A-1	60/F	11	+1	+2	+1	+3	+3	–	+1	+2	+4	–	+1	+4	+4	–	+1	+4	+4	–	+1	+1	+1	+1
A-2	59/M	13	0	+2	0	–	+1	–	0	+4	+4	–	+2	+4	–	–	+4	+2	–	–	+2	+1	+2	+1
A-3	67/M	18	0	+1	+3	+4	+4	–	0	+3	+4	–	+2	+3	+2	–	+3	+3	+4	+4	+2	+1	+2	+2
A-4	83/F	25	+2	+2	+2	+4	+4	–	0	+3	+4	–	+1	+4	+3	+4	0	+4	+4	–	+2	+2	+1	+2
A-5	71/F	26	0	+3	+2	+4	+4	–	–	+4	+4	–	+1	+4	+3	+4	0	+4	+4	–	+2	+2	+1	+1
A-6	58/M	28	0	+1	+3	+4	+4	–	–	+4	+4	–	+1	+4	+3	+4	0	+4	+4	–	+2	+1	+2	+2
A-7	51/M	32	+3	+3	+2	+4	+4	–	0	+4	+4	–	0	+4	+3	–	+2	+4	+4	–	+2	+1	+2	+1
A-8	61/F	36	+1	+1	–	+3	–	–	–	+4	+4	–	+3	+4	+4	–	+2	+1	+4	–	+2	+1	+2	+1
A-9	61/F	53	0	+1	–	+4	+4	–	–	+4	+4	–	+2	–	+3	–	0	+4	+4	–	+2	+2	+2	+2
A-10	68/M	60	+3	+3	+1	+4	+4	–	+2	+3	+3	–	+2	+3	+2	–	+1	+4	+4	–	+2	+2	+2	+2
A-11	68/M	72	+1	0	–	+3	–	–	–	+4	+4	–	+1	+4	+4	–	+1	+4	+4	–	+2	+1	+2	+2
A-12	53/M	72	0	0	–	–	–	–	–	–	–	–	–	+4	+4	–	+4	+4	–	–	+2	+2	+1	+2
A-13	69/F	79	0	0	–	+4	–	–	–	+4	–	–	–	–	–	–	–	–	+4	–	+2	+2	+1	+1
A-14	50/M	96	0	0	–	–	–	–	–	–	+4	–	–	–	–	–	–	–	+4	–	+2	+2	+2	+2
A-15	83/F	144	0	0	+4	+4	+4	–	–	+4	+4	–	–	+4	+4	–	–	+4	+4	–	+2	+2	+1	+1
Control cases		Causes of death																						
C-1	61/M	HCC	0	0	+3	+4	–	–	+3	–	–	–	+3	–	–	–	+3	–	–	–	0	0	0	0
C-2	61/M	Lung cancer	0	0	+3	–	–	–	+2	–	–	–	+2	–	–	–	+1	+4	–	–	0	0	0	0
C-3	62/M	HCC	0	0	+3	–	–	–	+3	+4	–	–	+3	+4	–	–	+3	+4	–	–	0	0	0	0
C-4	71/F	CRF	0	0	+2	–	+4	–	+2	+4	+4	–	+2	–	–	–	+2	+4	+4	–	0	0	0	0
C-5	86/F	Lung cancer	0	0	+2	–	–	–	+1	+4	+4	–	+2	+4	+4	–	+2	+4	–	–	0	0	0	0

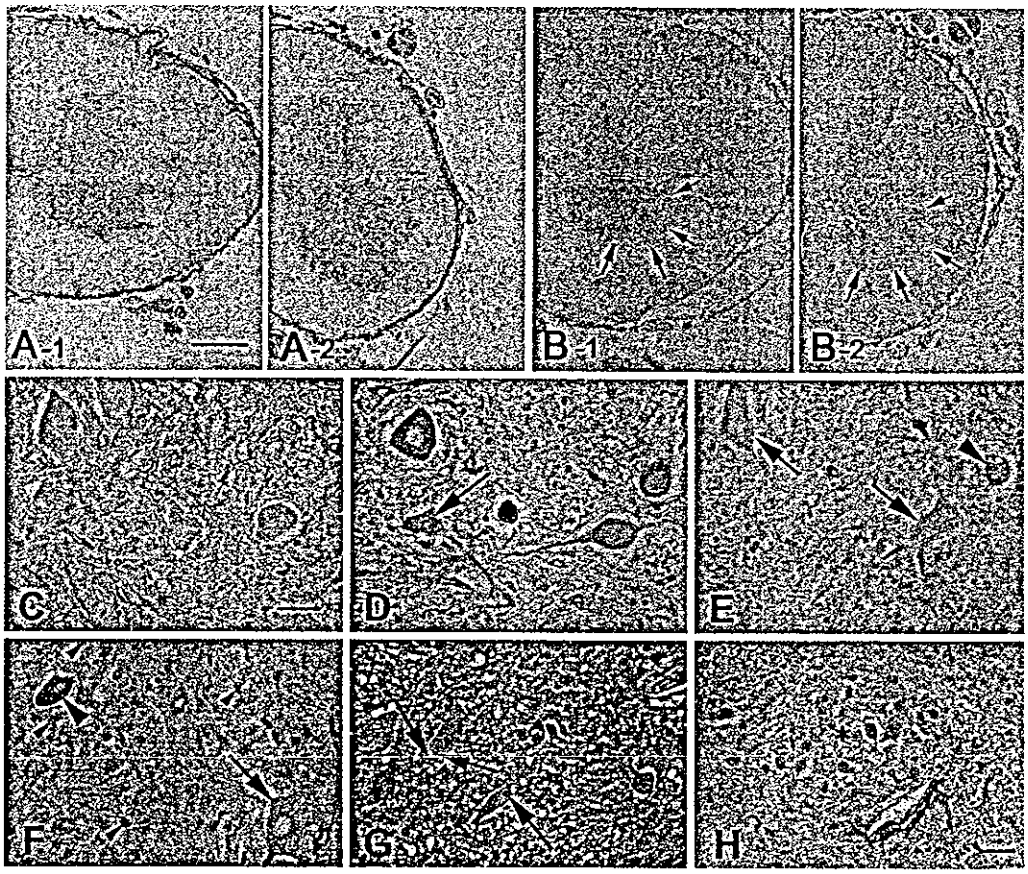

Materials and methods

Tissue source

This study was carried out using spinal cords obtained at autopsy from 15 cases of adult-onset sporadic ALS (average age of 64.1 years) and 5 control cases (average age of 68.2 years). The postmortem interval ranged from 2 to 21 h (average 5.4 h). The clinical characteristics of ALS and control cases are summarized in Table 1.

The spinal cords were stored at –80°C for biochemical analyses, or fixed for several weeks in buffered 10% formalin and then embedded in paraffin for pathological examinations. After embedding, 6-μm-thick sections were prepared. For the routine neuropathological study, the sections were stained with hematoxylin-eosin, Bodian's stain and Klüver-Barrera stain. The pathology at the sixth cervical level (C6) and the third lumbar level (L3) of the spinal cord were evaluated.

Antibodies

The immunohistochemistry (IHC) and Western blotting (WB) were performed using an anti-human cystatin C rabbit polyclonal antibody (DAKO, 1:500 for IHC, 1:1,000 for WB), an anti-human cathepsin B rabbit polyclonal antibody (Ab-3, Calbiochem, 1:200 for IHC and WB), an anti-human cathepsin H goat polyclonal antibody (N-18, Santa Cruz, 1:200 for IHC and WB), an anti-human cathepsin L goat polyclonal antibody (S-20, Santa Cruz, 1:200 for IHC and WB), an anti-human cathepsin D rabbit polyclonal antibody (Upstate Biotechnology, 1:200 for IHC and Ab-2, Calbiochem, 1:200 for WB), an anti-neuron-specific enolase (NSE) mouse monoclonal antibody (DAKO, 1:200 for WB) and an anti-glial fibrillary acidic protein (GFAP) rabbit polyclonal antibody (DAKO, 1:1,000 for IHC).

Fig. 1 Immunohistochemistry for cathepsin B in the C6 (**A-1, B-1**) and L3 (**A-2, B-2**) of either a control case (**A, C** case C-3) or ALS cases (**B, D, E, G** case A-7; **F** case A-11; **H** case A-12). **A** Immunoreactivity to cathepsin B in the control case is present in the gray matter in both cervical (**A-1**) and lumbar (**A-2**) spinal cord. **B** Cathepsin B immunoreactivity in ALS cases is preferentially decreased at the ventro-lateral side of the anterior horn (surrounded by *arrows*) in both the cervical (**B-1**) and lumbar (**B-2**) spinal cord. **C** Cathepsin B immunoreactivity is detected in the neuropil and cytoplasm of some anterior horn cells. Positive neurons and negative neurons are distributed randomly in the control case. **D** Cathepsin B immunoreactivity is increased in shrunken neurons (*arrow*) at the medial division of the anterior gray horn in an ALS case. **E** Cathepsin B immunoreactivity is decreased in the neuropil and normal-appearing motor neurons (*arrows*), but is increased in a pigmented neuron (*arrowhead*) at the lateral division of the anterior gray horn in an ALS case. **F** Cathepsin B immunoreactivity is increased in a shrunken neuron (*large arrowhead*) and reactive astrocytes (*small arrowheads*), but decreased in the normal-appearing neuron (*arrow*) of severe lesions in ALS case. **G** Double immunostaining for cystatin C (*grayish blue*) and cathepsin B (*brown*). The cathepsin B immunoreactivity is decreased in neurons bearing Bunina bodies (*arrows*). **H** Immunoreactivity of cathepsin B is increased in several small vessels but is reduced in the Onuf nucleus (*asterisk*) (case A-12) (*ALS* amyotrophic lateral sclerosis, *C6/L3* sixth cervical/third lumbar spinal cord levels). *Bars* **A-1** (also for **B-1, -2**) 1 mm; **C** (also for **D–G**) 50 μm; **H** 50 μm

Immunohistochemistry

IHC was performed using an indirect immunoperoxidase method as in previous reports [20, 21]. After blocking the endogenous peroxidase activity with methanol, sections were autoclaved at 120°C for 10 min to enhance the immunoreactivity and incubated with the

antibodies overnight at 4°C. The sections were then washed and incubated for 1 h with the horseradish peroxidase-conjugated anti-rabbit (PI-1000), anti-mouse (PI-2000) or anti-goat (PI-9500) antibodies (Vector Laboratories, USA) diluted by 1:200. The colored reaction product was developed with 3,3'-diaminobenzidine tetrahydrochloride. Double immunostaining was carried out for cystatin C and cathepsin B as described previously [20].

We divided the anterior gray horn into medial (MAG) and lateral (LAG) parts as described in the previous report [20, 21]. We counted the number of anterior horn cells on the right side of the C6 and L3 spinal cord in each specimen.

Western blot analysis for cathepsins

Approximately 30 mg tissue from the anterior horn of lumbar spinal cords was homogenized in 2% SDS, 2 mM EDTA, 2 mM PMSF and 50 mM TRIS-HCl (pH 6.8). Immunoblotting was carried out according to the previous method [22]. Proteins (20 μg/lane) were electrophoresed on 12% SDS-polyacrylamide gel and transferred onto a PVDF membrane (Millipore). The blots were reacted with the primary antibodies specific for cathepsins B, H, L and D, and then reacted with the corresponding secondary antibodies (dilution 1:10,000). The cathepsin signals were made visible using an ECL system (Amersham).

Results

Immunohistochemistry

Immunohistochemical findings are summarized in Table 1 and Fig. 2.

Cathepsin B

Controls. The gray matter of the spinal cords displayed diffuse immunostaining for cathepsin B (Fig. 1A). Cathepsin B-immunopositive motor neurons were randomly distributed in the anterior horns (Fig. 1C). The proportion of positive motor neurons was approximately 40% (Fig. 2A, C).

ALS cases. Immunoreactivity of cathepsin B was weakened in the LAG of several ALS cases (Fig. 1B). Normal-appearing, shrunken, pigmented and chromatolytic neurons were detected in a mosaic pattern as previously reported [16, 20].Cathepsin B immunoreactivity was increased in shrunken and pigmented neurons and several normal-appearing neurons in the MAG (Fig. 1D) as well as in shrunken and pigmented neurons and also reactive astrocytes in LAG (Fig. 1E). On the other hand, it was negative or faintly positive in the neuropil and a few normal-appearing neurons of the LAG (Fig. 1E). The remaining normal-appearing neurons tended to be negative to cathepsin B, especially in the severely affected region of the anterior horn in ALS cases (Fig. 1F). There were two patterns of cathepsin B immunoreactivity in anterior horn cells: moderately to strongly positive cathepsin B (cathepsin B-high) and negative to faintly positive cathepsin B (cathepsin B-low) in ALS, and we analyzed these two patterns in anterior horn cells (Fig. 2). The proportion of cathepsin B-high, normal-appearing neurons in ALS cases (C6: range 0–67%, average 23%, Fig. 2B; L3: range 0–54%, average 31%, Fig. 2D) was lower than in control cases (C6: range 8–62%, average 42%, Fig. 2A; L3: range 25–55%, average 42%, Fig. 2C), although the difference was not significant (C6: P=0.16 and L3: P=0.36). Notably, cathepsin B positivity was particularly low or absent in the normal-appearing neurons containing Bunina bodies (Fig. 1G). The number of cathepsin B-positive cells containing Bunina bodies among the various types of anterior horn cells in ALS cases (cases A-2, -4, -6, -7, -9, -10) was: 2/10 (20%) (cathepsin B positive cells/total cells containing Bunina bodies) at C6, and 2/13 (15%) at L3 in normal-appearing neurons, 4/4 (100%) and 2/2 (100%) in shrunken neurons, and 5/8 (63%) and 10/10 (100%) in pigmented neurons. The cathepsin B immunoreactivity was decreased in Onuf

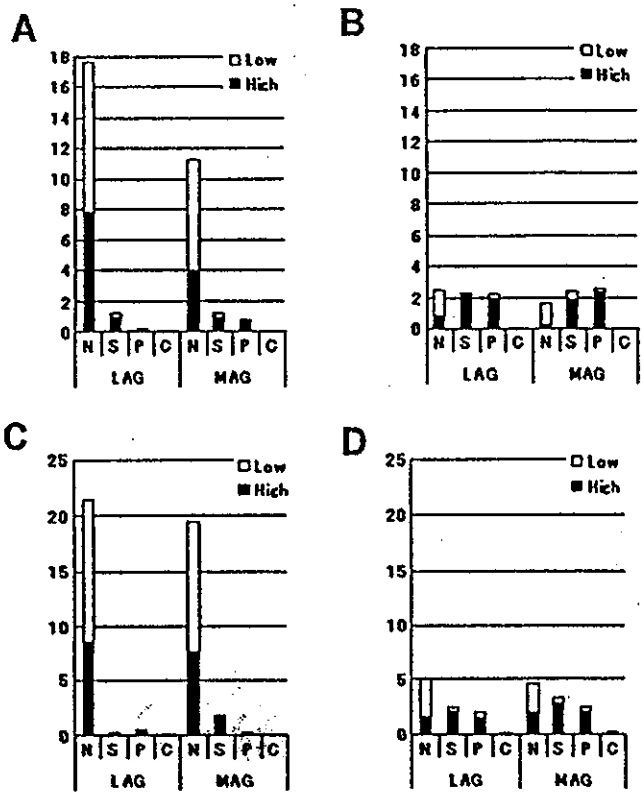

Fig. 2 The number of cathepsin B-high (moderately to strongly positive) anterior horn cells of the C6 (A, B) and the L3 (C, D) in the control (A, C) and ALS (B, D) cases. The total number of anterior horn cells (cell number shown in Y-axis) decreased in ALS cases in comparison with control cases. In ALS, normal appearing neurons (*N* in X-axis) decrease remarkably, while both shrunken (*S* in X-axis) and pigmented (*P* in X-axis) neurons increase in the C6 (B) and the L3 (D) spinal cords. The average proportion of cathepsin B-high normal-appearing neurons is 41% in the C6 (A) and 40% in the L3 (C) in control cases, respectively. The averaged proportion of cathepsin B-high anterior horn neurons in the C6 (B) and L3 (D) in ALS is 23% in C6 and 31% in L3 in normal-appearing neurons, 90% in C6 and L3 in shrunken neurons, and 92% in C6 and 89% in L3 in pigmented neurons, respectively. The number of the chromatolytic neurons (*C* in X-axis) in both control and ALS cases is small, but they are usually positive for cathepsin B. "High" in the figure indicates moderate to strongly immunopositive to cathepsin B and "Low" indicates completely immunonegative to faintly immunopositive to cathepsin B (*LAG* lateral division of anterior gray horn, *MAG* medial division of anterior gray horn)

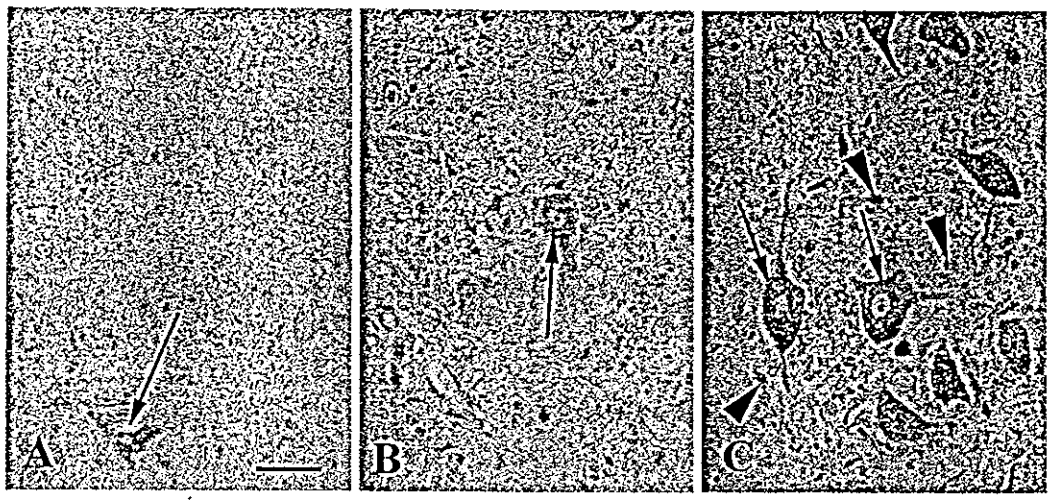

Fig. 3 Immunohistochemistry for cathepsin H (A, case A-7), cathepsin L (B, case A-7) and cathepsin (C, case A-11) in the L3 of ALS cases. A Aggregated lipofuscin granules in an anterior horn cell are immunolabeled with cathepsin H (*arrow*), whereas other normal-appearing neurons are not. B Aggregated lipofuscin granules in an anterior horn cell are immunolabeled with anti-cathepsin L antibody (*arrow*), whereas other normal-appearing neurons are immunonegative. C The cathepsin D immunoreactivity is elevated in the cytoplasm of all motor neurons (*arrows*) and several astrocytes (*arrowheads*). *Bar* A (also for B, C) 50 μm

nuclei as well as in 5 of the 6 ALS cases examined (cathepsin B immunoreactivity of Onuf nuclei was decreased in cases A-1, -5, -9, -12, -13 but not case A-6) (Fig. 1H).

Cathepsins H and L

Cathepsins H and L were expressed in lipofuscin granules in a few anterior horn cells in ALS (Fig. 3A, B) or control cases (data not shown). There was no significant difference between ALS and control cases.

Cathepsin D

Cathepsin D was expressed in the cytoplasm of all anterior horn cells in both control and ALS cases (Fig. 3C). There was no significant difference between control and ALS cases. Several reactive astrocytes were positive for cathepsin D in all ALS cases (Fig. 3C).

Western blot analysis of cathepsins B, H, L and D

Both the pro-enzyme form (43 kDa) and the activated form (31 kDa) of cathepsin B signals were often detected in both ALS and control cases (Fig. 4A). The other activated form of cathepsin B molecules (25 kDa) was detected in control cases and one of the ALS cases examined. Signals of the activated (34 kDa) and pro-enzyme (52 kDa) forms of cathepsin D were also detected in both ALS and control cases (Fig. 4B). The signals for NSE (44 and 46 kDa) were decreased in ALS cases, which indicated that the remaining neurons in the anterior horn were few in ALS cases (Fig. 4C). On the other hand, signals for cathepsin H (26 kDa) and cathepsin L (30 kDa) were hardly detected in either ALS or control cases (Fig. 4D, E).

Discussion

Among the lysosomal enzymes, cathepsin B distribution differed significantly between ALS and control cases. There were two distinct populations, showing high or low immunoreactivity to cathepsin B, in the anterior horn cells of the controls. In ALS, however, this pattern of cathepsin B expression in the anterior horn cells was modified. Most normal-appearing neurons showed relatively lower immunoreactivity, while abnormal-appearing neurons showed higher immunoreactivity to cathepsin B. In addition, reactive astrocytes were also immunolabeled by the anti-cathepsin B antibody in ALS cases. Western blot analyses of the spinal cord tissue showed that the 31-kDa activated form of cathepsin B occurred frequently in ALS cases in spite of the decrease in the numbers of neurons, especially in those cases that showed moderate to severe gliosis (Table 1). These results indicated that this 31-kDa form of cathepsin B could be derived not only from neurons but also from reactive astrocytes in ALS. In addition, the signal of the 25-kDa-activated form of cathepsin B was not detected in two of the three ALS cases examined and was detected to a lesser extent in the other ALS case (in which NSE was relatively preserved), compared with the control. Thus, the 25 kDa-activated form of cathepsin B might be down-regulated according to the degree of neuronal cell degeneration. The 25 kDa-activated form of cathepsin B may be closely associated with the population of motor neurons. Recently, Felbor et al. [11] reported that cathepsin B- and L-lacking mice showed neuronal loss, brain atrophy and lysosomal inclusion bodies in large cortical neurons. They asserted that cathepsin B and L have a role in maintenance of the central nervous system. Although we did not find cathepsin L signals in motor neurons of the spinal cord, our result is considered to be consistent with their report.

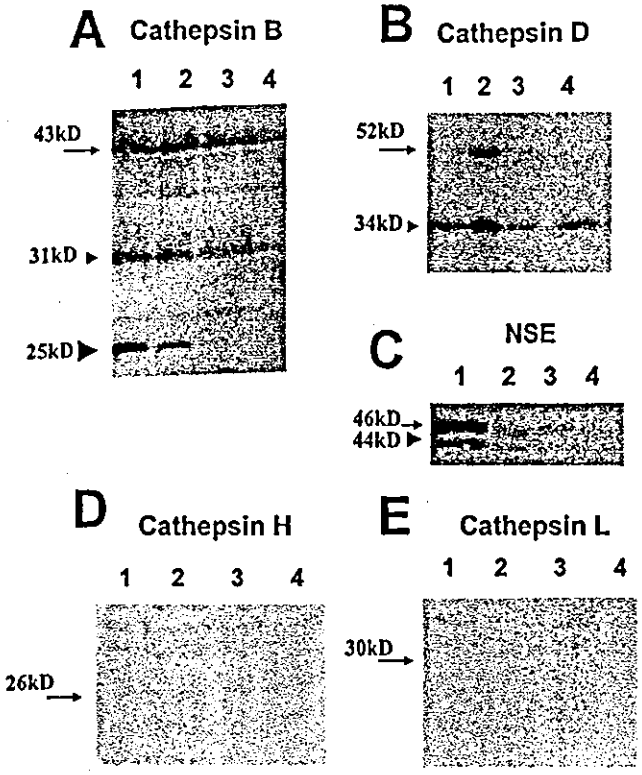

Fig. 4 Western blot analysis of cathepsin B (A), cathepsin D (B), NSE (C), cathepsin H (D) and cathepsin L (E) in control cases (*lane 1* case C-5) and ALS cases (*lane 2* case A-14, *lane 3* case A-13, *lane 4* case A-10). A Signals of the pro-enzyme form (43 kDa, *arrow*) and the activated form (31 kDa, *small arrowhead*) of cathepsin B are detected in both control and ALS cases. Another activated form of cathepsin B (25 kDa, *large arrowhead*) is noted in control (*lane 1*) and weakly detected in one ALS case (*lane 2*). B Signals of the pro-enzyme form of cathepsin D (41 kDa, *arrow*) are detected in control (*lane 1*) and two ALS cases (*lanes 2* and *3*). Signals of an activated form of cathepsin D (34 kDa, *arrowhead*) are detected in all control and ALS cases. C Signals of NSE (44 kDa, *arrowhead* and 46 kDa, *arrow*) as an internal standard of the spinal motor neurons are readily detected in the controls, but not or only faintly in ALS cases. D Signals of cathepsin H (26 kDa, *arrow*) is hardly detected in either control or ALS cases. E Signals of cathepsin L (30 kDa, *arrow*) is hardly detected in either control or ALS cases. (*NSE* neuron-specific enolase)

Cathepsins B, H and L are lysosomal cysteine proteases, while cathepsin D belongs to the aspartic proteases and activates pro-enzyme forms of cathepsins B, D, H and L [28]. There have been several reports on cathepsins, especially cathepsins B and D, in various neurological diseases [5, 6, 9, 13, 15, 17, 27]. Ii et al. [17] reported that cathepsin B immunoreactivity increased at the site of intracellular neurofibrillary tangles, degenerative neurites and dendrites in and outside senile plaques of AD brain. Cataldo et al. [9] also reported that immunoreactivity of cathepsins B and D, and β-hexoaminidase increased at the degenerated sites of AD brain in the early stage. Hill et al. [15] reported that cathepsin B immunoreactivity increased in CA1 neurons of the hippocampus in the rat two-vessel occlusion model of global ischemia. These data suggested that cathepsin B is strongly associated with neuronal cell death. Several authors reported that apoptosis occurs during the neurodegeneration process in ALS [33], and cathepsin B is also known to be associated with apoptosis. Shibata and colleagues [19, 35] reported that cathepsin B suppressed apoptotic cell death in a cultured PC12 cell line, while Vancompernolle et al. [36] reported that cathepsin B regulated caspase-11 and induced nuclear apoptosis. Kingham et al. [23] reported that activated microglia could trigger neuronal apoptosis, which may be mediated through the secretion of cathepsin B. Our results also suggest that cathepsin B could be associated with the neurodegeneration process of the motor neurons. It is noteworthy that cathepsin B expression was lower in the normal-appearing neurons containing Bunina bodies, which may indicate that Bunina bodies attenuate cathepsin B accumulation in the remaining normal-appearing motor neurons. In addition, cathepsin B expression was low or absent in Onuf nuclei, spared in ALS, while it was constantly high in the shrunken and pigmented neurons. These results suggest that motor neurons expressing less cathepsin B might be resistant to the pathological process of ALS.

With respect to the expression of cathepsin in the glial cells, cathepsin B immunoreactivity was high in the cytoplasm of reactive astrocytes in our study, consistent with the previous reports [5, 6, 27]. Nakamura et al. [27] reported that some reactive astrocytes were positively stained with the antisera against cathepsins B and D in brains of AD cases. Bever et al. [6] showed that monocytes, macrophages and reactive astrocytes are potential sources of increased cathepsin B in multiple sclerosis brains. Recently, several authors implicated an involvement of inflammatory processes in ALS [1, 3, 37]. Cathepsin B is also involved in the inflammatory process in various diseases [12, 24] and activates the proinflammatory caspase-11, which may induce the inflammation associated with glial reaction [34]. Our results suggest that reactive astrocytes may play a crucial role in the cathepsin B-mediated motor neuronal cell degeneration in ALS. There are also several reports concerning the up-regulation of cathepsin D in either neurons or glial cells of neurodegenerative diseases including AD [13, 26, 29]. Further examination of the glial expression of cathepsins in ALS remains necessary.

In conclusion, among the cathepsins we examined, only the expression of cathepsin B was increased in the degenerative neurons of ALS. We therefore propose that cathepsin B may play an important role in the motor neuron degeneration of ALS.

Acknowledgements A part of this study was carried out at the Morphology Core, Graduate School of Medical Sciences, Kyushu University. This work was supported by a grant of the Nakabayashi Trust for ALS research.

References

1. Almer G, Guegan C, Teismann P, Naini A, Rosoklija G, Hays AP, Chen C, Przedborski S (2001) Increased expression of the pro-inflammatory enzyme cyclooxygenase-2 in amyotrophic lateral sclerosis. Ann Neurol 49:176–185

2. Alves-Rodrigues A, Gregori L, Figueiredo-Pereira ME (1998) Ubiquitin, cellular inclusions and their role in neurodegeneration. Trends Neurosci 21:516–520
3. Appel SH, Smith RG, Alexianu MF, Engelhardt JI, Stefani E (1995) Autoimmunity as an etiological factor in sporadic amyotrophic lateral sclerosis. Adv Neurol 68:47–57
4. Barrett AJ, Davis ME, Grubb A (1984) The place of human γ-trace (cystatin C) against the cysteine proteinase inhibitors. Biochem Biophys Res Commun 120:631–636
5. Bernstein HG, Keilhoff G, Kirschke H, Wiederanders B, Rinne A, Khudoerkov R, Dorn A (1986) Cathepsins B and D in rat brain glia during experimentally induced neuropathological defects. An immunocytochemical approach. Biomed Biochim Acta 45:1461–1464
6. Bever CT Jr, Garver DW (1995) Increased cathepsin B activity in multiple sclerosis brain. J Neurol Sci 131:71–73
7. Bond JS, Butler PE (1987) Intracellular proteases. Annu Rev Biochem 56:333–364
8. Bunina TL (1962) On intracellular inclusions in familial amyotrophic lateral sclerosis. Korsakov J Neuropathol Psychiatry 62:1293–1299
9. Cataldo AM, Hamilton DJ, Nixon RA (1994) Lysosomal abnormalities in degenerating neurons link neuronal compromise to senile plaque development in Alzheimer disease. Brain Res 640:68–80
10. Cookson M, Shaw P (1999) Oxidative stress and motor neuron disease. Brain Pathol 9:165–186
11. Felbor U, Kessler B, Mothes W, Goebel HH, Ploeggh HL, Bronson RT, Olsen BR (2002) Neuronal loss and brain atrophy in mice lacking cathepsin B and L. Proc Natl Acad Sci USA 99:7883–7888
12. Gerber A, Welte T, Ansorge S, Buhling F (2000) Expression of cathepsins B and L in human lung epithelial cells is regulated by cytokines. Adv Exp Med Biol 477:287-292
13. Ginsberg SD, Hemby SE, Lee VM, Eberwine JH, Trojanowski JQ (2000) Expression profile of transcripts in Alzheimer's disease tangle-bearing CA1 neurons. Ann Neurol 48:77–87
14. Gutman L, Mitsumoto H (1996) Advances in ALS. Neurology (Suppl 2) 47:S17–S18
15. Hill IE, Preston E, Monette R, MacManus JP (1997) A comparison of cathepsin B processing and distribution during neuronal death in rats following global ischemia or decapitation necrosis. Brain Res 751:206–216
16. Hirano A (1982) Aspects of the ultrastructure of amyotrophic lateral sclerosis. Adv Neurol 36:75–88
17. Ii K, Ito H, Kominami E, Hirano A (1993) Abnormal distribution of cathepsin proteinases and endogenous inhibitors (cystatins) in the hippocampus of patients with Alzheimer's disease, parkinsonism-dementia complex on Guam, and senile dementia and in the aged. Virchows Arch [A] 423:185–194
18. Ince PG, Lowe J, Shaw PJ (1998) Amyotrophic lateral sclerosis: current issues in classification, pathogenesis and molecular pathology. Neuropathol Appl Neurobiol 24:104–117
19. Kanamori S, Waguri S, Shibata M, Isahara K, Konishi A, Kametaka S, Watabe T, Ebisu S, Kominami E, Uchiyama Y (1998) Overexpression of cation-dependent mannose 6-phosphate receptor prevents cell death induced by serum deprivation in PC12 cells. Biochem Biophys Res Commun 251:204–208
20. Kikuchi H, Doh-ura K, Kawashima T, Kira J, Iwaki T (1999) Immunohistochemical analysis of the spinal cord lesions in amyotrophic lateral sclerosis using microtubule associated protein 2 (MAP2) antibodies. Acta Neuropathol 97:13–21
21. Kikuchi H, Doh-ura K, Kira J, Iwaki T (1999) Preferential neurodegeneration in the cervical spinal cord of progressive supranuclear palsy. Acta Neuropathol 97:577–584
22. Kikuchi H, Furuta A, Nishioka K, Suzuki SO, Nakabeppu Y, Iwaki T (2002) Impairment of mitochondrial DNA repair enzymes against accumulation of 8-oxo-guanine in the spinal motor neurons of amyotrophic lateral sclerosis. Acta Neuropathol 103:408–414
23. Kingham PJ, Pocock JM (2001) Microglial secreted cathepsin B induces neuronal apoptosis. J Neurochem 76:1475–1484
24. Lang A, Horler D, Baici A (2000) The relative importance of cysteine peptidases in osteoarthritis. J Rheumatol 27:1970–1979
25. Lowe J (1994) New pathological findings in amyotrophic lateral sclerosis. J Neurol Sci 124 (Suppl):38–51
26. Mantle D, Falkous G, Ishiura S, Perry RH, Perry EK (1995) Comparison of cathepsin protease activities in brain tissue from normal cases and cases with Alzheimer's disease, Lewy body dementia, Parkinson's disease and Huntington's disease. J Neurol Sci 131:65–70
27. Nakamura Y, Takeda M, Suzuki H, Hattori H, Tada K, Hariguchi S, Hashimoto S, Nishimura T (1991) Abnormal distribution of cathepsins in the brain of patients with Alzheimer's disease. Neurosci Lett 130:195–198
28. Nishimura Y, Kawabata T, Yano S, Kato K (1990) Intracellular processing and activation of lysosomal cathepsins. Acta Histochem Cytochem 23:53–64
29. Nogami M, Takatsu A, Endo N, Ishiyama I (2000) An immunohistochemical study on cathepsin D in human hippocampus. Histochem J 32:505–508
30. Okamoto K, Hirai S, Amari M, Watanabe M, Sakurai A (1993) Bunina bodies in amyotrophic lateral sclerosis immunostained with rabbit anti-cystatin C serum. Neurosci Lett 162:125–128
31. Reiss C, Lesnik T, Parvez H, Parvez S, Ehrlich R (2000) Conformational toxicity and sporadic conformational diseases. Toxicology 153:115–121
32. Rowland LP (2000) Hereditary and acquired motor neuron disease. Spinal cord disease. In: Rowland LP. (ed) Merritt's neurology, 10th edn. Lippincott, Williams & Wilkins, Philadelphia, pp 703–707
33. Sathasivam S, Ince PG, Shaw PJ. (2001) Apoptosis in amyotrophic lateral sclerosis: a review of the evidence. Neuropathol Appl Neurobiol 27:257–274
34. Schotte P, Van Criekinge W, Van de Craen M, Van Loo G, Desmedt M, Grooten J, Cornelissen M, De Ridder L, Vandekerckhove J, Fiers W, Vandenabeele P, Beyaert R (1998) Cathepsin B-mediated activation of the proinflammatory caspase-11. Biochem Biophysical Res Commun 251:379–387
35. Shibata M, Kanamori S, Isahara K, Ohsawa Y, Konishi A, Kametaka S, Watanabe T, Ebisu S, Ishido K, Kominami E, Uchiyama Y (1998) Participation of cathepsin B and D in apoptosis of PC12 cells following serum deprivation. Biochem Biophys Res Commun 251:199–203
36. Vancompernolle K, Herreweghe FV, Pyneart G, Craen MV de, Vos KD, Totty N, Sterling A, Fiers W, Vandenabeele P, Grooten J (1998) Atractyloside-induced release of cathepsin B, a protease with caspase-processing activity. FEBS Lett 438: 150–158
37. Yasojima K, Tourtellotte WW, McGeer EG, McGeer PL (2001) Marked increase in cyclooxygenase-2 in ALS spinal cord: implications for therapy. Neurology 57:952–956

Probable Sporadic Creutzfeldt-Jakob Disease with Valine Homozygosity at Codon 129 and Bilateral Middle Cerebellar Peduncle Lesions

Takashi NISHIDA*·****, Aya M. TOKUMARU**, Katsumi DOH-URA***, Akira HIRATA*, Kazuo MOTOYOSHI* and Keiko KAMAKURA*

Abstract

We describe a 67-year-old *Japanese* man with probable sporadic Creutzfeldt-Jakob disease (CJD) who had valine homozygosity at codon 129, a rarity in the Japanese. T2-weighted magnetic resonance imaging (MRI) detected high-intensity lesions in the bilateral middle cerebellar peduncles and basal ganglia as well as cerebellar and cortical atrophy. He developed cerebellar ataxia and subsequent mental deterioration, myoclonus, and periodic synchronous discharge as shown in an electroencephalogram. Cerebrospinal fluid examination showed a high level of neuron-specific enolase and a positive immunoassay for the 14-3-3 protein. He died of pneumonia 10 months after the initial symptoms appeared. Whether or not the genetic polymorphism increased his susceptibility to sporadic CJD is not clear because valine homozygosity at codon 129 is less than 1% in the normal Japanese population. Although there is no convincing evidence in the present case, the MRI findings of cerebellar peduncle changes, which are rare in CJD, suggest a kind of degeneration, demyelination, or both.
(Internal Medicine 42: 199–202, 2003)

Key words: cerebellar ataxia, codon 129 polymorphism, susceptibility

Introduction

Creutzfeldt-Jakob disease (CJD) is characterized by dementia, myoclonus, and periodic synchronous discharge (PSD) seen in electroencephalograms (EEG). Valine homozygosity at codon 129 of the prion protein (PrP) gene is a rare polymorphism in Japan (1, 2), whereas it has been reported to confer genetic predisposition to sporadic CJD in England and Germany (3, 4). High signal intensities in the bilateral middle cerebellar peduncles on T2-weighted magnetic resonance imaging (MRI) are reported to be MRI features in intoxication and neurodegenerative diseases, but not CJD (5–7). We present a case of probable sporadic CJD for which PrP gene analysis found valine homozygosity at codon 129 and brain MRI showed high-intensity signal abnormalities in the bilateral middle cerebellar peduncles on T2-weighted images obtained in the late phase of illness.

Case Report

A 67-year-old retired pharmacist was admitted to our hospital in January 1998 because of slowly progressive cerebellar symptoms of double vision, ataxic speech, and unsteady gait of 6 months duration. Just before admission, he became confined to a wheelchair due to severe gait disturbance. His past history showed he had had Wallenberg's syndrome in March 1996. External hemorrhoidectomy and appendectomy had been performed under spinal anesthesia respectively about 20 and 30 years earlier. He had had hypertension since age 50. He had no past history of blood transfusions or acupuncture. His father had died of heart failure, and his mother of myocardial infarction.

Physical examination at admission yielded the following data: blood pressure, 182/118 mmHg; temperature, 37.1°C; pulse rate, 88 beats/minute. No anemia, jaundice, or swollen lymph nodes were observed, nor abnormal findings for the lungs, heart and abdomen. His score on the Revised Version of Hasegawa's dementia scale was 23 (full score 30), but evaluation was difficult due to severe ataxic dysarthria.

From *the Third Department of Internal Medicine, **Department of Radiology, National Defense Medical College, Tokorozawa, ***Department of Neuropathology, Neurological Institute, Graduate School of Medical Sciences, Kyushu University, Fukuoka and ****Department of Parasitology, National Defense Medical College, Tokorozawa

Received for publication July 24, 2002; Accepted for publication November 25, 2002

Reprint requests should be addressed to Dr. Keiko Kamakura, Internal Medicine III, National Defense Medical College, 3-2 Namiki, Tokorozawa, Saitama 359-8513

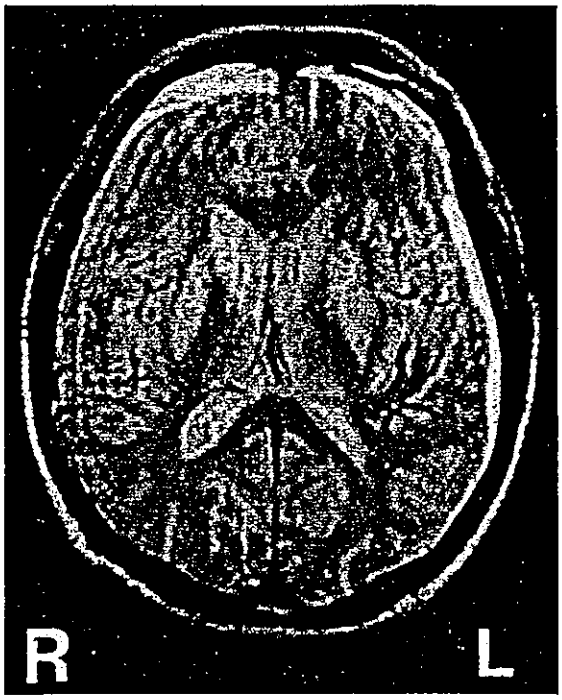

Figure 1. Cranial MRI on admission showing bilateral hyperintensity in the caudate nuclei and putamina on T2-weighted sequences (TR 3,500 ms, TE 19 ms).

Neurological examination revealed ataxic speech, truncal ataxia, severe limb ataxia, and normoreflexia in the lower extremities, but no pathological reflexes. There were no signs of limb muscle weakness or sensory disturbance. He was unable to stand or walk because of severe ataxia. Laboratory test findings were total bilirubin, 1.0 mg/dl (normal; 0.2–1.2); aspartate aminotransferase (AST), 33 IU/*l* (normal; 8–30); alanine aminotransferase (ALT), 30 IU/*l* (normal; 5–35); lactate dehydrogenase (LDH), 208 IU/*l* (normal; 100–225); blood urea nitrogen, 12 mg/dl; serum creatinine, 1.0 mg/dl; Na, 142 mEq/*l*; K, 3.8 mEq/*l*; Cl, 104 mEq/*l*; Ca, 9.4 mg/dl. Cerebrospinal fluid (CSF) findings showed a normal cell count, 61 mg/dl total protein (normal, 10–40); 67 mg/dl glucose (normal, 50–75); 88 ng/ml neuron-specific enolase (NSE) (normal, ≦10); and a positive immunoassay for the 14-3-3 protein. CSF cytology was class 2. Analysis of the PrP gene showed valine homozygosity at codon 129. He had no mutations at PrP codons 102, 105, 117, 145, 178, 180, 200, 210, 219, or 232. Single photon emission computed tomography detected diffusely decreased regional cerebral blood flow of 30–36-ml/100 g/minute with no perfusional defect.

Repeated MRI and angiography done before admission did not find any abnormalities, including in the cerebellum and basal ganglia, although his severe cerebellar symptoms slowly worsened. Cranial MRI on admission, 6 months after the initial symptoms appeared, showed bilateral hyperintensity in the caudate nuclei and putamina on T2-weighted sequences for the first time and isointensity on T1-weighted images without contrast enhancement (Fig. 1). Moreover, mild cerebellar atrophy had first been pointed out by the radiologist. However, cortical atrophy had not been noted at that time. Bilateral chronic subdural hematomas also were present. As his mental status had deteriorated slowly, we made the tentative diagnosis of possible prion disease based on clinical findings of progressive consciousness disturbance, ataxia of cerebellar origin, high NSE in the CSF, the absence of a family history, and MRI features. Intravenous hyperalimentation was started at the end of January due to worsening of his dysphagia and consciousness disturbance. A follow-up MRI study on the 42nd hospital day showed progressive atrophic changes in the cerebellum and basal ganglia, particularly in the caudate nuclei heads. In addition, the frontotemporal region of the cerebrum appeared atrophic. Clonazepam was administered to control myoclonus in his upper extremities, which developed in February. A follow-up EEG in April detected PSD (Fig. 2). The last MRI examination on the 114th day showed bilateral lesions in middle cerebellar peduncles (Fig. 3). Cortical atrophy, predominantly of the fronto-temporal region, was present, and his severe cerebellar atrophy had worsened. In addition, the putamina showed a high signal intensity on the T1-weighted images and isointensity on the T2-weighted sequences, probably because of the administration of total parenteral nutrition. He died of pneumonia in May 1998.

Discussion

Our *Japanese* patient presented cerebellar symptoms at onset followed by consciousness disturbance and myoclonus after 7 months and PSD after 9 months during a clinical course of about 10 months. In addition, none of the PrP gene mutations already reported were found. According to the recently established molecular basis for phenotypic heterogeneity of sporadic CJD, six different phenotypes are characterized by the size of the protease-resistant fragment of the pathological PrP (types 1 and 2) and homozygosity or heterozygosity for methionine or valine at codon 129 of the PrP gene (designated by MM1, MM2, MV1, MV2, VV1, and VV2). Zerr et al (8) reported 2 cases of VV1 patients and 15 cases of VV2 patients; VV1 patients differed from VV2 patients by younger age at onset (range of 23–31 years vs median of 62 years and range of 40–76 years) and by longer disease duration (range of 20–31 months vs median of 7.5 months and range of 2.9–15.7 years). Regarding this point, the present patient's age at onset and disease duration was similar to those of VV2 patients. A necropsy, however, could not be performed on our patient because of hospital policy. Cerebellar ataxia at onset and hyperintensities in the basal ganglia, which were also seen in our case, were observed in 47% and 70% of VV2 patients, respectively. However, no VV2 patients had myoclonus or PSD in the EEG. On the other hand, Miyazono et al (9) reported that in Japanese sporadic CJD, the change in the PrP codon 129 affects the

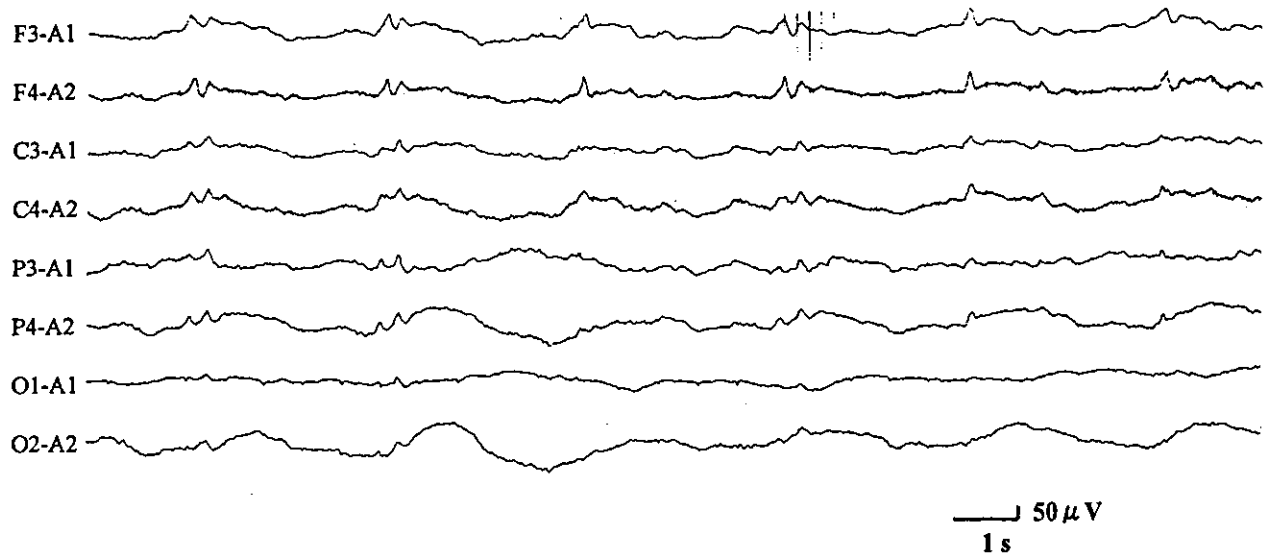

Figure 2. EEG detected PSD at intervals of about 3.0–4.0 seconds.

clinical course. They examined one CJD patient who had valine homozygosity and six CJD patients who had valine heterozygosity at PrP codon 129 (Val/Val and Met/Val CJD patients). For comparison, they also examined 13 sporadic CJD patients with methionine homozygosity at codon 129 (Met/Met CJD patients) and 7 GSS patients who had leucine instead of proline at PrP codon 102. In comparison to Met/Met CJD patients, Val/Val and Met/Val CJD patients had a relatively long clinical duration (a mean of 33 months) and ataxia at onset, but rarely PSD on their EEGs. The clinicopathological findings for Val/Val and Met/Val CJD were similar to those for GSS, but immunohistochemistry findings showed different PrP deposit distributions and morphologies.

There are significant differences regarding genetic polymorphism at PrP codon 129 in the populations of Japan, England, and Germany (1–4). In England and Germany where normal subjects with valine homozygotes make up more than 10% of the populations (3, 4), valine homozygosity at codon 129 may increase susceptibility to sporadic CJD. The frequency of valine homozygosity at codon 129 found for 179 normal, unrelated Japanese is much lower (no Val/Val, 15 Met/Val and 164 Met/Met) (1). Any predisposition to sporadic CJD therefore would be masked in Japan if a patient has valine homozygosity at PrP codon 129 (1), as did our patient. Whether his genetic polymorphism increased the risk of probable sporadic CJD remains a matter of speculation.

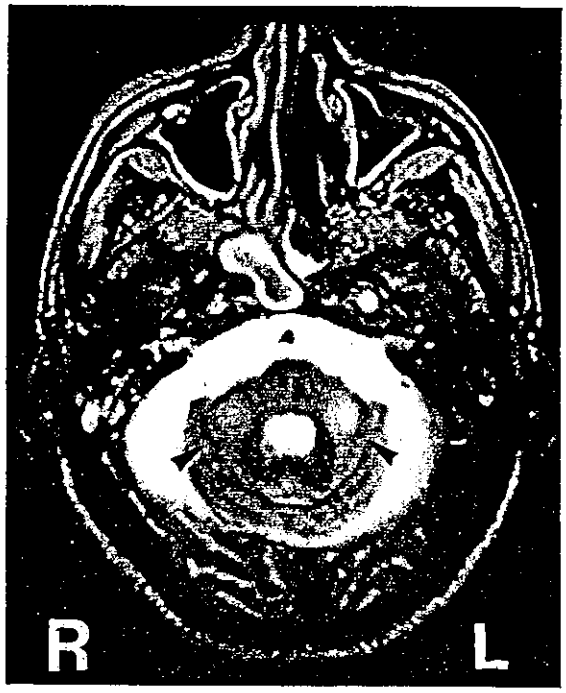

Figure 3. Cranial MRI showing bilateral lesions of the middle cerebellar peduncles as a high signal intensity on the T2-weighted image (arrowheads).

MRI findings for CJD are lesions such as cortical atrophy, cerebellar atrophy, and hyperintensity at the basal ganglia as seen on T2-weighted images (10–12). In the present case, cranial MR T2-weighted images already had revealed high signal intensities in the bilateral caudate nuclei and putamina before definite cognitive impairment developed. Moreover, brain MRI showed abnormal signal intensities in the bilateral middle cerebellar peduncles late in the course of the illness. To our knowledge, similar findings have never been reported for sporadic CJD. On the other hand, similar lesions in the

middle cerebellar peduncles are reported to be a radiological feature in chronic toluene intoxication, multiple system atrophy, portal-systemic shunt encephalopathy, and citrullinemia (5–7). In the case of chronic toluene intoxication, similar MRI findings are presumed to be demyelinating lesions (6). Regarding multiple system atrophy, the high intensity areas on the T2-weighted images, including the middle cerebellar peduncles, suggest degeneration and demyelination (7). Although there was no pathological evidence, the MRI features in this case suggest a kind of degeneration, demyelination, or both at the middle cerebellar peduncles.

We presented the case of a Japanese man with probable sporadic CJD who had a rare polymorphism of codon 129 Val/Val, and an additional rare finding of high intensity in the cerebellar peduncle on T2-weighted MR images.

References

1) Doh-ura K, Kitamoto T, Sakaki Y, Tateishi J. CJD discrepancy. [letter; comment] Nature 353: 801–802, 1991.
2) Yamauchi K, Tateishi J. Slow Virus Infection and Prion Disease. Kindai Shuppan, Japan, 1994: 214–226 (in Japanese).
3) Schulz-Schaeffer WJ, Giese A, Windl O, Kretzschmar HA. Polymorphism at codon 129 of the prion protein gene determines cerebellar pathology in Creutzfeldt-Jakob disease. Clin Neuropathol 15: 353–357, 1996.
4) Windl O, Dempster M, Estibeiro JP, et al. Genetic basis of Creutzfeldt-Jakob disease in the United Kingdom: a systematic analysis of predisposing mutations and allelic variation in the PRNP gene. Hum Genet 98: 259–264, 1996.
5) Hitoshi S, Terao Y, Mizuno T, Takeda K, Sakuta M. A case of portal-systemic encephalopathy presenting characteristic MR images in globus pallidus, hypothalamus, corpus callosum, pontine base, and middle cerebellar peduncle. Rinsho Shinkeigaku (Clin Neurol) 32: 217–219, 1992 (in Japanese, Abstract in English).
6) Suzuki K, Wakayama Y, Takada H, Okayasu H. A case of chronic toluene intoxication with abnormal MRI findings: abnormal intensity areas in cerebral white matter, basal ganglia, internal capsule, brain stem and middle cerebellar peduncle. Rinsho Shinkeigaku (Clin Neurol) 32: 84–87, 1992 (in Japanese, Abstract in English).
7) Yagishita T, Kojima S, Hirayama K. MRI study of degenerative process in multiple system atrophy. Rinsho Shinkeigaku (Clin Neurol) 35: 126–131, 1995 (in Japanese, Abstract in English).
8) Zerr I, Schulz-Schaeffer WJ, Giese A, et al. Current clinical diagnosis in Creutzfeldt-Jakob disease: identification of uncommon variants. Ann Neurol 48: 323–329, 2000.
9) Miyazono M, Kitamoto T, Doh-ura K, Iwaki T, Tateishi J. Creutzfeldt-Jakob disease with codon 129 polymorphism (valine): a comparative study of patients with codon 102 point mutation or without mutations. Acta Neuropathol 84: 349–354, 1992.
10) Gertz HJ, Henkes H, Cervos-Navarro J. Creutzfeldt-Jakob disease: correlation of MRI and neuropathologic findings. Neurology 38: 1481–1482, 1988.
11) Milton WJ, Atlas SW, Lavi E, Mollman JE. Magnetic resonance imaging of Creutzfeldt-Jacob disease. [see comments] Ann Neurol 29: 438–440, 1991.
12) Barboriak DP, Provenzale JM, Boyko OB. MR diagnosis of Creutzfeldt-Jakob disease: significance of high signal intensity of the basal ganglia. AJR Am J Roentgenol 162: 137–140, 1994.

Acta Neuropathol (2003) 106 : 92–96
DOI 10.1007/s00401-003-0697-y

CASE REPORT

Kensuke Sasaki · Katsumi Doh-ura · Akiko Furuta
Sachi Nakashima · Yumi Morisada · Jun Tateishi
Toru Iwaki

Neuropathological features of a case with schizophrenia and prion protein gene P102L mutation before onset of Gerstmann-Sträussler-Scheinker disease

Received: 21 November 2002 / Revised: 3 February 2003 / Accepted: 3 February 2003 / Published online: 8 April 2003

Abstract Gerstmann-Sträussler-Scheinker disease (GSS) is a hereditary transmissible spongiform encephalopathy associated with prion protein gene mutation P102L. The age of onset is roughly restricted to around the sixth decade; however, it is unclear whether the disease-specific pathology of GSS is already evident in the pre-clinical stage. We had a chance to examine an autopsy case with PRNP P102L mutation. The patient had died at 50 years of age before the clinical symptoms of GSS had appeared; neither neuronal loss, gliosis nor spongiform change was found anywhere in the brain. Immunohistochemistry failed to detect any deposition of prion protein. It is thus considered that amyloid plaque formation in GSS probably develops in a relatively rapid fashion compared with Alzheimer's disease. Although the patient suffered from schizophrenia, no significant pathological changes were detected except for astrocytic inclusion bodies in the cerebral cortex. The nature and significance of the inclusion bodies, which are not observed in patients with GSS, remain unclear.

Keywords Creutzfeldt-Jakob disease · Gerstmann-Sträussler-Scheinker syndrome · Glial inclusion · Prion disease · Schizophrenia

K. Sasaki (✉) · K. Doh-ura · A. Furuta · T. Iwaki
Department of Neuropathology, Neurological Institute, Graduate School of Medical Sciences, Kyushu University, 812-8582 Fukuoka, Japan
Tel.: +81-92-6425539, Fax: +81-92-6425540,
e-mail: ksasaki@np.med.kyushu-u.ac.jp

S. Nakashima · Y. Morisada
Kurashiki Neurological Hospital, Okayama, Japan

J. Tateishi
Brain Research Laboratory,
Harukaze Geriatric Health Care Facilities, Fukuoka, Japan

Introduction

Gerstmann-Sträussler-Scheinker disease (GSS) is a hereditary transmissible spongiform encephalopathy associated most commonly with a mutation at codon 102 of the prion protein gene (PRNP) from proline to leucine [3, 5, 7]. The principal clinical features of GSS are prominent cerebellar ataxia and dementia, which develops gradually. Pathological features are characterized by kuru plaque-type prion protein (PrP) deposition, neuronal loss and gliosis in the cerebellar and cerebral cortices [2, 12]. The age of onset is roughly restricted to around the sixth decade; however, it is unclear whether the disease-specific pathology develops gradually, starting long before any clinical signs appear, or is manifested in a relatively rapid fashion around the onset of disease. We examined an autopsy case with PRNP P102L mutation, where the patient had committed suicide at 50 years of age, before any of the clinical symptoms of GSS had appeared. In the present case, disease-specific pathological features were not manifested in the pre-clinical stage.

Case report

The present case is patient II-3 in the pedigree shown in Fig. 1. At the age of 17 years, her scholastic achievement at high school rapidly deteriorated. At 20 years of age, she was taken into protective custody because she had begun to wander about wearing an inane smile and talking incoherently. Her disease was diagnosed as schizophrenia and she underwent psychiatric treatment. From then on she was occasionally admitted to hospital whenever her persecutory-reference delusion worsened. She was finally permanently hospitalized when she was 32 years old. Signs of autism, dissociable affection, ambivalent feeling and loosening of association were continuously observed. No neurological signs such as cerebellar ataxia, myoclonus or dementia were observed. She sometimes attempted suicide and, at the age of 50 years, she succeeded in committing suicide by ingesting synthetic detergent; she died from pulmonary edema.

Patient I-5, the father of this case, developed cerebellar ataxia at 53 years of age and had become bed-ridden by the age of 58. He died at 61 years of age and an autopsy was performed. His brain weighed 1,170 g. Histochemically, numerous congophilic plaques